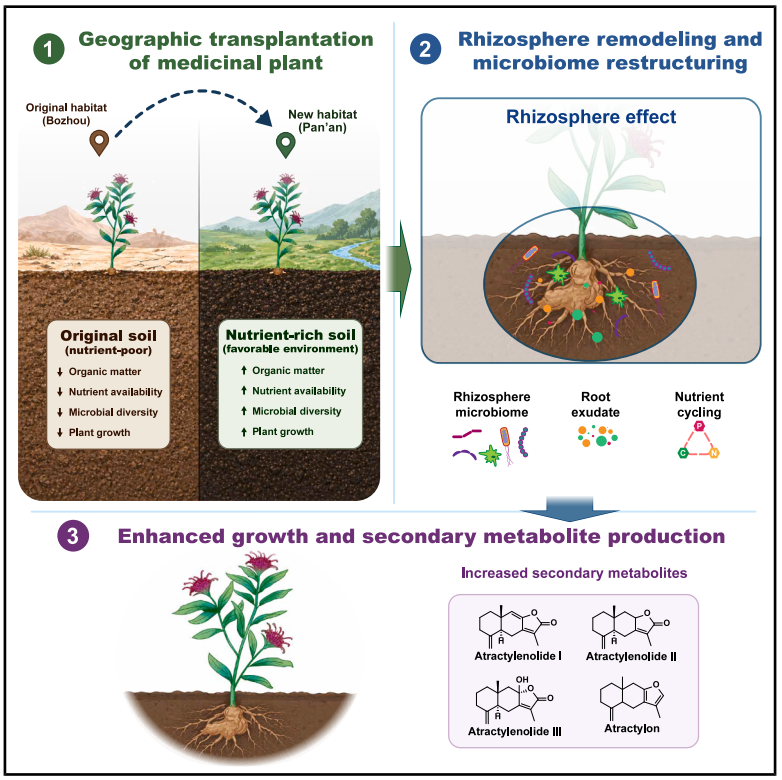
iScience

Article

Geographic transplantation promotes the growth of *Atractylodes macrocephala* by restructuring the rhizosphere microbial community

Graphical abstract



Highlights

- *Atractylodes macrocephala* from Bozhou grew better after transplanted to Pan'an
- Transplantation altered the structure and diversity of the rhizosphere microbiome
- Eleven upregulated core genera correlated with enhanced metabolic functions

Authors

Yuchen Ping, Yue Peng, Jian Sun, ..., Cong Dang, Jiangjie Lu, Dawei Xue

Correspondence

lujj@hznu.edu.cn (J.L.), dwxue@hznu.edu.cn (D.X.)

In brief

Soil science; Ecology

Ping et al., 2026, iScience *29*, 116350
July 17, 2026 © 2026 The Author(s). Published by Elsevier Inc.
https://doi.org/10.1016/j.isci.2026.116350

CellPress

iScience

CellPress
OPEN ACCESS

Article

Geographic transplantation promotes the growth of *Atractylodes macrocephala* by restructuring the rhizosphere microbial community

Yuchen Ping,[1,6] Yue Peng,[1,6] Jian Sun,[2,3] Jinxi Xiang,[1] Pan Wang,[4] Yanghui Shen,[4] Jiayou Xia,[5] Cong Dang,[1,3] Jiangjie Lu,[1,3,*] and Dawei Xue[1,3,7,*]

[1]College of Life and Environmental Sciences, Zhejiang Provincial Key Laboratory for Genetic Improvement and Quality Control of Medicinal Plants, Hangzhou Normal University, Hangzhou 311121, China
[2]Innovation Center of Chinese Medicine Crops, Institute of Horticulture, Zhejiang Academy of Agricultural Sciences, Hangzhou 310021, China
[3]Zhejiang Provincial Modern Biology and Medicine Industry College, Hangzhou 310023, China
[4]Pan'an Traditional Chinese Medicine Industry Innovation and Development Institute, Pan'an 322300, China
[5]Hangzhou Dipont School of Arts and Science, Hangzhou 310057, China
[6]These authors contributed equally
[7]Lead contact
*Correspondence: lujj@hznu.edu.cn (J.L.), dwxue@hznu.edu.cn (D.X.)
https://doi.org/10.1016/j.isci.2026.116350

SUMMARY

This study systematically elucidated the microecological mechanisms underlying *Atractylodes macrocephala* geoherbalism via integrated transplantation experiments across China's four major producing regions. Data showed that soil from Pan'an significantly enhanced the accumulation of bioactive compounds in *A. macrocephala* sourced from Bozhou. 16S rRNA gene sequencing revealed that geographic transplantation significantly restructured the rhizosphere microbial community and markedly increased its α-diversity. Functional metabolic analysis indicated that transplantation to Pan'an regulated various pathways and enhanced secondary metabolism in the rhizosphere microbiome. Co-occurrence network analysis revealed 11 upregulated keystone genera that potentially promoted secondary metabolism in *A. macrocephala*, and were positively correlated with root growth and bioactive compound accumulation. These results demonstrate that direct soil nutrient supply, microbiome-mediated C/N metabolism remodeling, and resource reallocation collectively drive *A. macrocephala* geo-authenticity. It will lay the groundwork for the use of microbiome biofertilizers and the cross-regional eco-cultivation of geo-authentic herbs.

INTRODUCTION

Atractylodes macrocephala is a critically important medicinal plant in traditional Chinese medicine (TCM) and is one of the "Zhejiang Eight TCM Herbs." Modern pharmacological research has not only has validated its traditional efficacy in fortifying the spleen, replenishing "Qi", promoting diuresis, and resolving dampness, but has also further revealed its multitarget mechanisms of action, including antitumor effects, immunoregulatory activities, and amelioration of metabolic syndrome.[1–4] With the increasing global demand for natural medicines surging, the cultivation area of *A. macrocephala* continues to expand. However, significant quality variations persist across different production regions. The content of bioactive compounds, notably, atractylenolides I–III and polysaccharides in its rhizomes, directly affects the clinical value and market competitiveness of the herb. This geographical divergence is intrinsically linked to regional heterogeneity in soil microecosystems.[5–7]

The soil ecosystem serves as the core interface for medicinal plant-environment interactions, and the regional heterogeneity of its physicochemical properties can influence the secondary metabolism of medicinal plants. Studies have shown that soil mineral elements (sodium, zinc, barium, and titanium) significantly affect the quality of *Polygonum multiflorum* medicinal materials by regulating the metabolism of stilbene glycosides and anthraquinones, leading to geographical divergence.[8] Rosemary essential oil yield is strongly correlated with parameters such as soil pH, calcium carbonate content, and the nitrogen-to-phosphorus ratio.[9] Moreover, the regulatory role of microbial communities in the rhizosphere microecosystem should not be neglected. As the "second genome" of plants, the rhizosphere microbiome participates in the regulation of secondary metabolism through pathways such as nutrient supply, signal transduction, and horizontal gene transfer. For example, soil-dwelling *Burkholderia*, which possesses plant symbiotic and stress-resistant functions, is considered a potential microbial agent that can indirectly influence medicinal material quality.[10] In soil environments with relatively low nitrogen contents, plants can recruit more nitrogen-fixing bacteria (such as *Paenarthrobacter* and *Sphingomonas*) by secreting palmitic acid, alleviating soil

This is an open access article under the CC BY-NC-ND license (http://creativecommons.org/licenses/by-nc-nd/4.0/).

nutrient deficiency and promoting plant growth.[11] Terpenoids are the most diverse and chemically variable natural compounds in plants and constitute active components of many medicinal plants.[12] Rhizosphere microbes activate terpene synthesis and promote monoterpene accumulation through interactions with the immune system of *Citrus reticulata*.[13]

Current research on the soil microbiota of *A. macrocephala* predominantly relies on laboratory-controlled conditions or single-production-region observations and fails to authentically reflect the dynamic mechanisms of environmental-biological factor interactions in agricultural ecosystems. Significant knowledge gaps persist, particularly in terms of the following dimensions: (1) how geographical isolation effects and soil factors synergistically drive spatial divergence patterns of microbial diversity in geo-authentic (a core concept in traditional Chinese medicine that describes the superior and consistent quality, specific chemical profile, and enhanced clinical efficacy of a medicinal material produced in a specific region, resulting from the unique combination of local genotype, environmental conditions, and cultivation practices) production regions; (2) whether conserved functional microbial taxa exist across different ecotypes of geo-authentic production regions and their niche conservation characteristics; and (3) the structural features of microbe-soil interaction networks in the root-rhizosphere microzone and their regulatory pathways for the biosynthesis of atractylenolide bioactive compounds. To address this, in this study selects four geo-authentic medicinal material production regions, Pan'an and Tiantai in Zhejiang Province, Bozhou in Anhui Province, and Enshi in Hubei Province were selected as research objects. By integrating multidimensional soil factor analysis and 16S rRNA amplicon sequencing, we constructed a coupled analytical framework of ''geographical environment-microbiome-medicinal components''. This approach will help elucidate how geographic divergence reshapes the rhizosphere microecosystem structures and elucidate the ecological functions of key microbial taxa in the accumulation of active medicinal components. Moreover, it will improve the ecological cultivation of Chinese medicinal herbs and sustainable industrial development.

RESULTS

Growth phenotype and active constituents of *A. macrocephala*

We evaluated the growth phenotypes and active component contents of *A. macrocephala* across seven treatment groups: PA_ES (Enshi samples planted in the Pan'an common garden), PA_BZ (Bozhou samples planted in the Pan'an common garden), PA (Pan'an), ES (Enshi), BZ (Bozhou), and TT (Tiantai).

Figure 1 illustrates that Bozhou-origin *A. macrocephala* planted in the Pan'an common garden (PA_BZ) exhibited the greatest growth vigor. In terms of plant height, the PA_BZ group significantly surpassed samples from other regions, except those from the BZ group. Branch number data reflected similar variations in growth performance (Figure 1B). Regarding root growth, both locally grown Bozhou samples and those transplanted into Pan'an exhibited significantly greater fresh root weight and root length compared to other treatment groups.

The contents of Atractylenolides I, II, and III, and Atractylon differed significantly among the treatment groups. Tiantai *A. macrocephala* contained higher levels of atractylenolide I and II but lower levels of atractylenolide III and Atractylon (Figure 2). Upon transplantation to Pan'an, Bozhou-origin *A. macrocephala* showed significant increases in all active components, marking the best performance for active compound accumulation (Figure 2).

Soil physicochemical properties across cultivation regions

The soil in the Pan'an region contained relatively high levels of total phosphorus and total potassium (Table 1). The Enshi region soil was slightly acidic and rich in organic matter and total nitrogen. In contrast, the Bozhou soil was near-neutral, with relatively low contents of organic matter, total nitrogen, and total potassium. The Tiantai soil, while similar in pH to the Pan'an soil, contained lower levels of organic matter, total nitrogen, and total potassium.

Diversity of rhizosphere and endophytic microorganisms associated with *A. macrocephala*

Community structure of the associated microbiota

Geographical transplantation and environmental differences significantly altered the taxonomic the structure of microbial communities in the rhizosphere, tuberous roots, and bulk soil.

In the rhizosphere, *Proteobacteria* dominated in the Pan'an, Enshi, and Tiantai groups (Figures 3D and 4A). The key genera included *Bradyrhizobium* in Pan'an and the *Burkholderia-Caballeronia-Paraburkholderia* complex in ES, which are associated with nitrogen fixation and secondary metabolite synthesis, respectively.[14,15] In the Bozhou rhizosphere, the dominant phylum *Actinobacteria* exhibited functional differentiation at the genus level. *Arthrobacter* and *Nocardioides* cooperatively adapt to the low organic matter environments. The former secretes plant growth hormones and increases antioxidant enzyme activity to alleviate oxidative stress, whereas the latter adsorbs heavy metals, thereby improving the plant's own detoxification capacity. In the *A. macrocephala* transplantation groups PA_ES and PA_BZ, the relative abundance of the phylum *Acidobacteria* increased. The abundance of its core taxon, *Candidatus Solibacter*, significantly increased in the relatively acidic environment, which is likely correlated with the soil pH conditions in Pan'an (Table 1).

The tuberous roots exhibited high conservation of *Proteobacteria*, represented primarily by the ubiquitous colonization of *Pseudomonas*. The unique presence of *Firmicutes* in PA_BZ, driven by *Lactobacillus*, decreased after transplantation, suggesting strict host selection of functional microbiota (Figures 3E and 4B). *Proteobacteria* and *Actinobacteria* dominated across all regions in the bulk soil microorganism community, but the abundance of *Chloroflexi* was significantly greater in the Tiantai group, possibly because of its relatively barren soil (Figures 3E and 4B).

These findings indicate that following geographic transplantation, the rhizosphere community of *A. macrocephala* was governed primarily by soil physicochemical properties (e.g., pH and organic matter), leading to restructuring at the phylum level. In contrast, the root endophytic community, which is

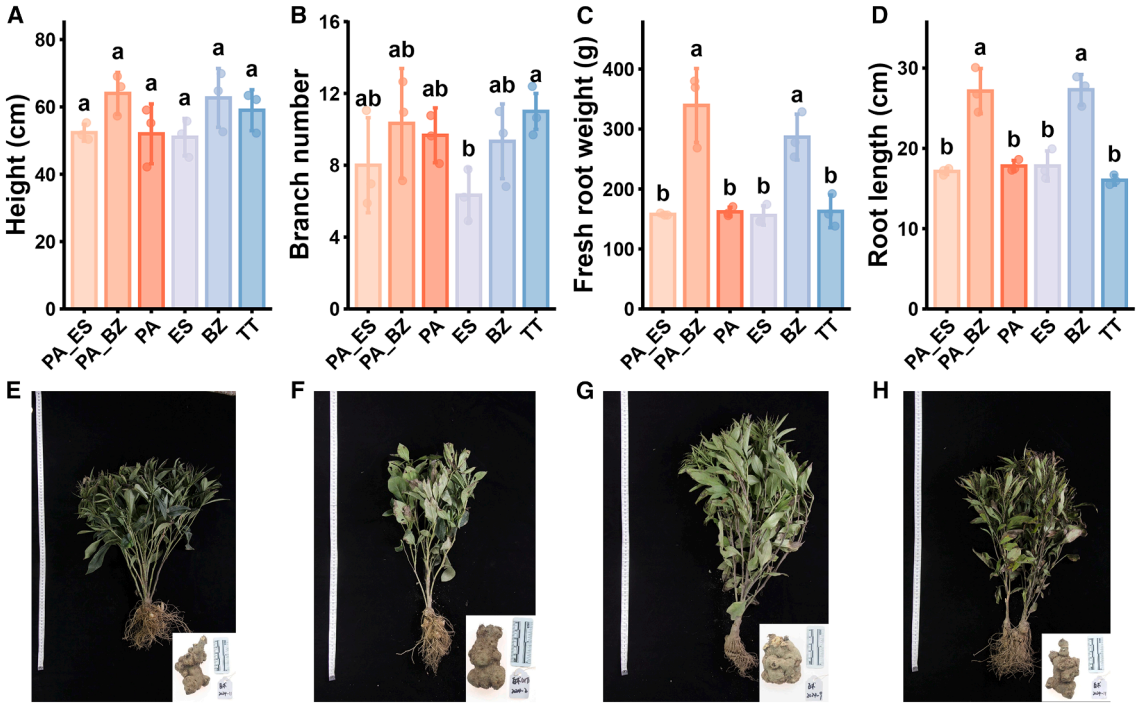


Figure 1. Bozhou-sourced *A. macrocephala* exhibits superior phenotypic traits when cultivated in Pan'an

(A) Plant height.

(B) Branch number.

(C) Fresh root weight.

(D) Root length.

PA_ES, plants f transplanted from Enshi into Pan'an homogeneous garden; PA_BZ, plants transplanted from Bozhou into Pan'an homogeneous garden; ES, Enshi; BZ, Bozhou; TT, Tiantai. Three biological replicates were established for each experimental group. Data were represented as mean ± SEM, and analyzed using one-way analysis of variance (ANOVA), and significant differences among means were further assessed with Duncan's multiple range test at a significance level of $p < 0.05$. Samples of *A. macrocephala* plants and tuberous roots were collected from (E) (Pan'an), (F) (Enshi), (G) (Bozhou), and (H) (Tiantai).

reliant on host metabolic regulation, maintained high conservation. Moreover, the bulk soil microbiota reflected a distinct trajectory of co-evolution, shaped by long-term environmental filtering and microbial functional adaptation, resulting in significant differences.

Intrinsic (alpha) diversity of the microbial communities

Geographic transplantation significantly affected rhizosphere alpha diversity. Compared with those in the original production areas, the Chao1 index, observed species number, Faith's phylogenetic diversity (Faith's PD), and Shannon index were significantly greater in the PA_ES and PA_BZ groups (Figure 5A). The PA_BZ group displayed the highest species richness and phylogenetic diversity. Simpson index analysis showed no significant dominant taxa in Pan'an-related treatment groups.

In contrast, the alpha diversity of the tuberous root endophytic community did not shift significantly after transplantation (Figure 5B). However, Bozhou-origin endophytic community maintained significantly higher Simpson dominance, Shannon diversity, and Pielou evenness than other groups. For bulk soil, the Tiantai samples presented the lowest diversity values (Figure 5C), while Enshi, Bozhou, and Pan'an showed comparable levels.

Comparative (beta) diversity of microbial communities

Principal coordinate analysis (PCoA) and non-metric multidimensional scaling (NMDS) analyses based on Bray-Curtis distance revealed that rhizosphere microbiomes of transplanted groups (PA_ES and PA_BZ) clustered closely with native Pan'an soils, separating significantly from their original regions (Figures 6A and 6D). The greatest dissimilarity occurred between Bozhou and Pan'an samples. Hierarchical clustering (Figure 6G) showed that the Pan'an transplantation groups had an even microbial distribution (Simpson dominance >0.99).

Beta diversity of tuberous root endophytes showed distinct clustering, with 90% of samples grouping tightly, except for specific outliers in the PA_BZ and Tiantai groups characterized by a surge in *Streptomyces* abundance (Figures 6B and 6E). *Pseudomonas* colonized the core community broadly (>40% relative abundance in >50% of samples). Bulk soil microbiomes showed complete separation among the four production areas (Figure 6C), with Bozhou soil displaying the distinct divergence (d > 0.98).

Correlations between rhizosphere microbes and phenotypes

To investigate changes in the rhizosphere microbial community of *A. macrocephala* across different geographic environments,

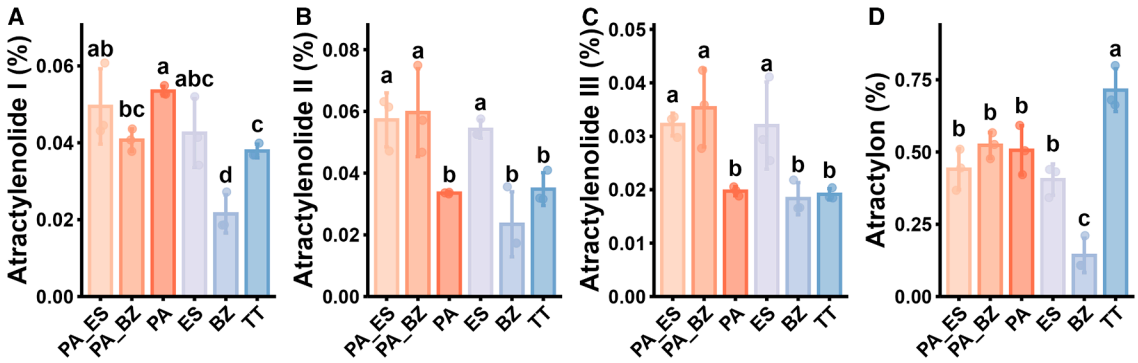


Figure 2. Bozhou-sourced *A. macrocephala* achieves the highest accumulation of active compounds when cultivated in Pan'an

(A) Atractylenolide I, (B) atractylenolide II, (C) atractylenolide III, (D) atractylon.

PA_ES, plants transplanted from Enshi into Pan'an homogeneous garden; PA_BZ, plants transplanted from Bozhou into Pan'an homogeneous garden; PA, Pan'an; ES, Enshi; BZ, Bozhou; TT, Tiantai. Three biological replicates were established for each experimental group. Data were represented as mean ± SEM, and analyzed using one-way analysis of variance (ANOVA), and significant differences among means were further assessed with Duncan's multiple range test at a significance level of $p < 0.05$.

a comparative analysis was conducted between samples from the native Bozhou site and Bozhou-sourced *A. macrocephala* transplanted to the Pan'an site. Using the random forest algorithm, genus-level microbial composition data were analyzed to identify microbial taxa with significant discriminatory power. Unclassified taxa were excluded, and the results were visualized alongside relative abundance changes (Figure S1).

The Random Forest model revealed that several microbial taxa significantly contributed to the classification between the native habitat group (BZ_RS) and the transplanted group (PA_BZ_RS). Among them, *Anaeromyxobacter*, *Armatimonadales*, and *Bauldia* presented relatively high Mean Decrease Gini values in the transplanted samples. Conversely, the use of genera such as *Kribbella*, *OM190*, and *Actinoplanes* had greater discriminatory power and significantly contributed to the model classification in the native habitat group. Further relative abundance analysis confirmed these findings, with statistically significant differences observed for these genera between the two groups. For instance, *Anaeromyxobacter* was significantly enriched in the transplanted group, whereas *Kribbella* was more abundant in the native habitat group.

We subsequently performed a Mantel analysis to evaluate the correlations between the differential bacterial genera (excluding unclassified taxa) identified via random forest analysis and the following variables: (1) key agronomic traits of *A. macrocephala* (plant height, branch number, root fresh weight, and root length), (2) characteristic secondary metabolites (atractylenolide I, II, III, and atractylon), and (3) soil physicochemical properties (pH, organic matter content, and available nitrogen, phosphorus, and potassium levels).

A Pearson correlation heatmap (Figure 8) revealed widespread positive correlations among the agronomic traits, particularly a greater degree of coupling between root length and both plant height and branch number, indicating a consistent growth trend in the plants post-transplantation. Conversely, most secondary metabolites were negatively correlated with growth traits, especially atractylenolide I, whose expression was inversely related to plant height and root length. The analysis of soil properties revealed a positive correlation between pH and plant growth, but a negative correlation with the accumulation of secondary metabolites. In contrast, organic matter content and the levels of nitrogen, phosphorus, and potassium showed opposite trends to pH, exhibiting positive correlations with the accumulation of active compounds.

As shown in Figure 8, several bacterial genera were correlated trends with either the morphogenesis or the accumulation of bioactive compounds in *A. macrocephala*. Among the significantly upregulated genera in the Pan'an environment compared with those in the Bozhou environment, *Anaeromyxobacter*, *Armatimonadales*, *Sphingomonas*, *Sulfuritalea*, *Tahibacter*, and *Tardiphaga* demonstrated strong positive correlations with multiple trait indicators. However, Mantel test analysis revealed an intriguing

Table 1. Soil pH, total organic matter, and inorganic element content of *Atractylodes albicans*

Region	pH	Total organic matter (g/kg)	Total nitrogen (mg/kg)	Total phosphorus (mg/kg)	Total potassium (mg/kg)
Pan'an	5.13 ± 0.06b	33 ± 1.01b	335.33 ± 28.49d	1,050 ± 65.57a	28,733.33 ± 676.59a
Enshi	4.76 ± 0.07c	75.63 ± 1.69a	3,636.67 ± 36.67a	737.67 ± 105.52b	22,666.67 ± 1791.03b
Bozhou	7.87 ± 0.09a	16.83 ± 0.13d	992.33 ± 34.48c	619 ± 36.56b	11,733.33 ± 1865.77c
Tiantai	4.52 ± 0.05days	26.87 ± 0.44c	1,230 ± 26.46b	711.67 ± 52.26b	19,900 ± 152.75b

Three biological replicates were established for each experimental group. Data were represented as mean ± SEM, and analyzed using one-way analysis of variance (ANOVA), and significant differences among means were further assessed with Duncan's multiple range test at a significance level of $p < 0.05$.

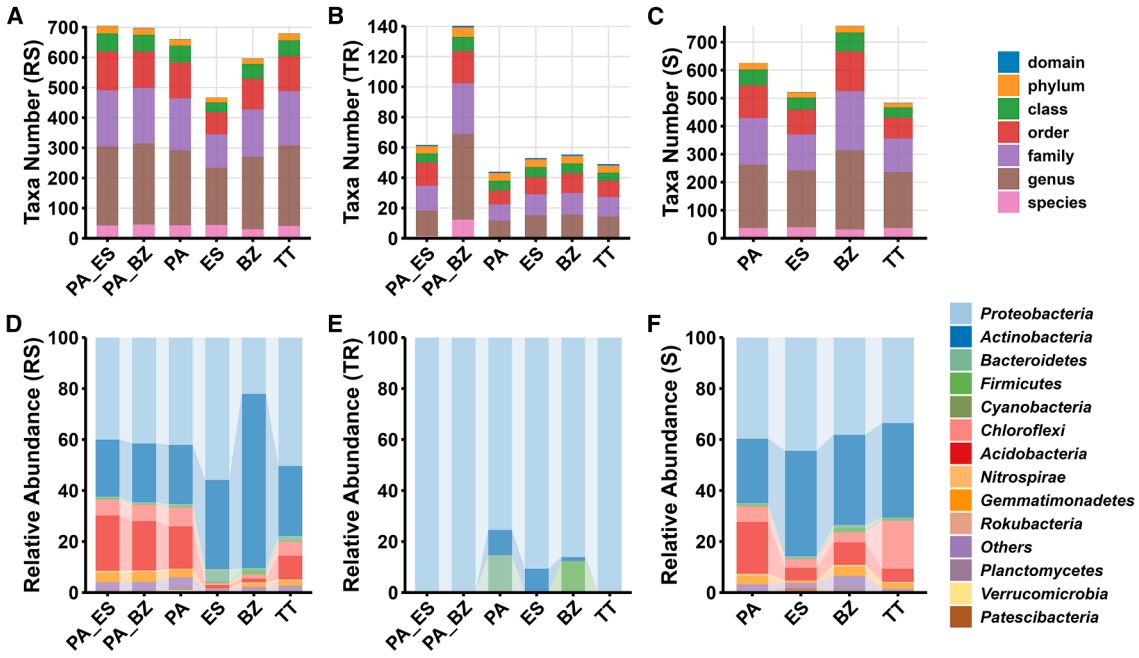


Figure 3. Species composition analysis (taxonomic unit count, taxonomic composition analysis

(A-C) Taxonomic unit count for rhizosphere (RS), tuberous roots (TR), and bulk soil (S), respectively.

(D-F) Taxonomic composition analysis for rhizosphere, tuberous roots, and bulk soil, respectively. (PA_ES, Enshi samples planted in the Pan'an common garden; PA_BZ, Bozhou samples planted in the Pan'an common garden; PA, Pan'an; ES, Enshi; BZ, Bozhou; TT, Tiantai).

phenomenon: the abundance of certain bacterial genera (such as *Actinoplanes*, *Glycomyces*, and *Saccharopolyspora*) significantly decreased in the PA environment despite their reduced abundance and exhibited positive correlations with the accumulation of multiple bioactive compounds in *A. macrocephala*. Notably, the actual contents of these compounds generally increased in Pan'an-transplanted plants.

Microbial metabolic pathways

Finally, we predicted microbial metabolic pathways to elucidate the metabolic functional restructuring of rhizosphere, tuberous root, and bulk soil microorganisms following the transplantation of *A. macrocephala* from its geo-authentic production area to Pan'an (Figure 8). Post-transplantation samples showed a general increase in biosynthetic pathway activity. Amino acid biosynthesis exhibited the greatest activity across all the samples. Carbohydrate and nucleotide degradation varied between groups; the TCA cycle maintained high overall activity, while glycolysis showed niche specificity. The rhizosphere community displayed the highest metabolic activity, particularly in aromatic compound degradation and oxidative phosphorylation. Bulk soil communities showed the highest fermentation activity but the lowest fatty acid and lipid synthesis. Tuberous root communities showed enhanced butyrate fermentation and methylglyoxal

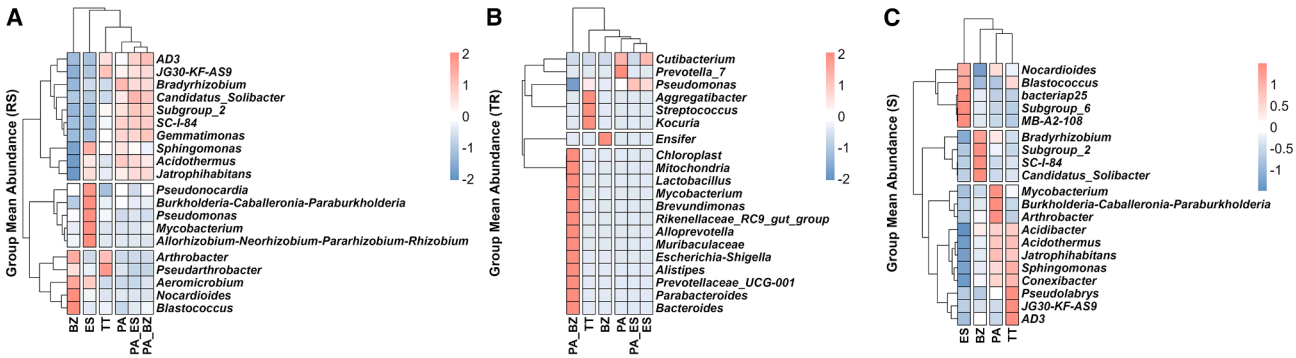
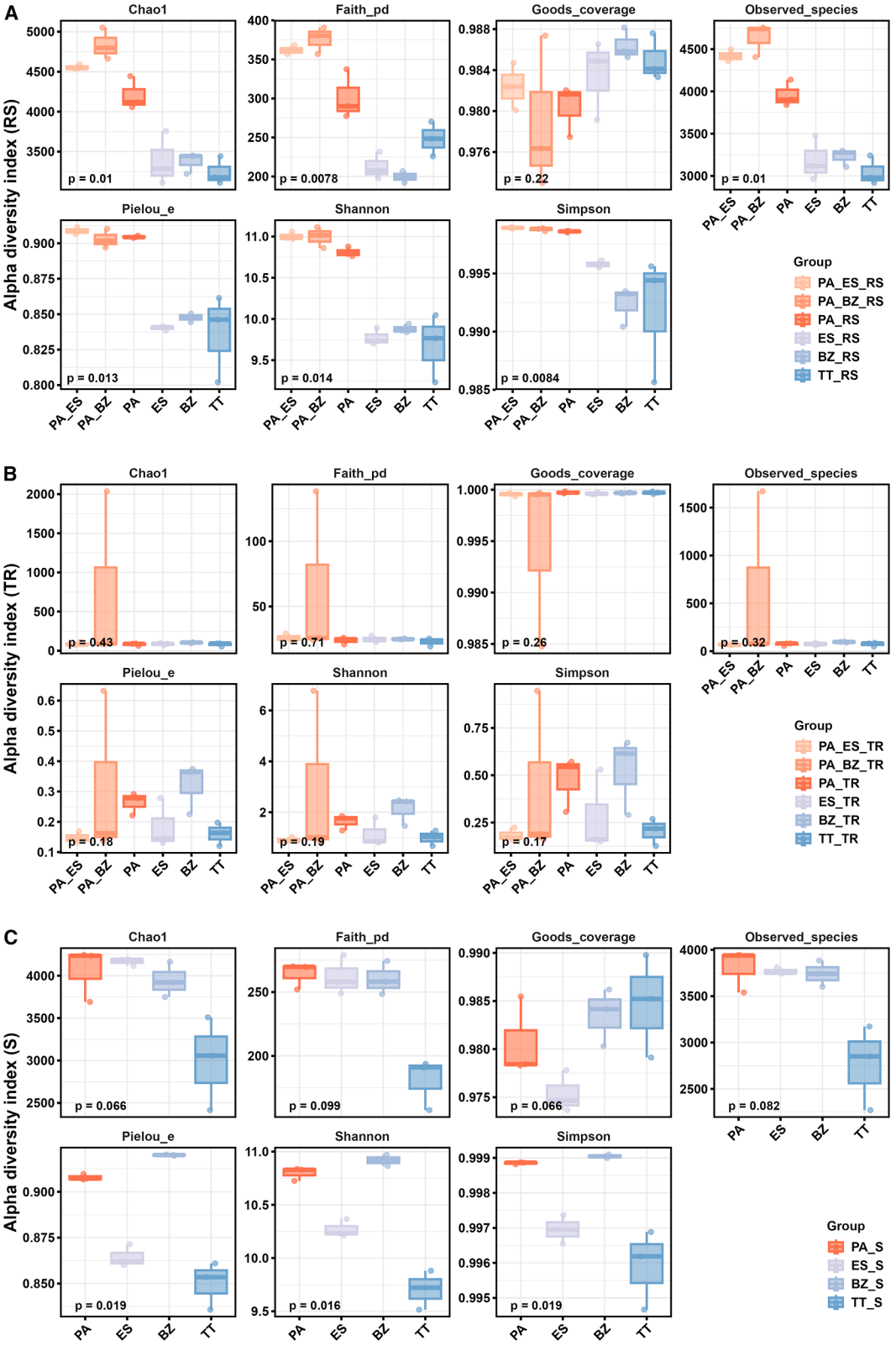


Figure 4. Heatmap of the species composition of soil and rhizosphere soil microorganisms of *Atractylodes macrocephala* in different regions

(A-C) Heatmaps of species composition for RS, TR, and S, respectively. RS, rhizosphere; TR, tuberous roots; S, bulk soil; PA_ES, Enshi samples planted in the Pan'an common garden; PA_BZ, Bozhou samples planted in the Pan'an common garden; PA, Pan'an; ES, Enshi; BZ, Bozhou; TT, Tiantai.



(legend on next page)

degradation pathways (METHGLYUT-PWY). Additionally, the enterobactin biosynthesis pathway (ENTBACSYN-PWY) was strongly upregulated in the Pan'an environment.

DISCUSSION

Soil conditions and microbial adaptation drive growth

Our results demonstrate that the growth and chemical composition of *A. macrocephala* depend heavily on local soil conditions. The robust growth observed in the PA_BZ group (Figure 1) correlates directly with the optimal soil pH and high phosphorus/potassium levels in the Pan'an region (Table 1). In contrast, the restricted growth in the ES group corresponds to limiting environmental factors, likely water and nutrient availability. The superior root development in Bozhou varieties indicates an inherent genetic advantage, which the favorable Pan'an soil conditions further amplified.

The soil environment is a key determinant of microbial community structure. Geographic transplantation disrupts the original ecological balance, resulting in a significant increase in rhizosphere alpha diversity (Figure 5A). The PA_BZ group showed the highest species richness, and its low Simpson dominance index indicates a shift toward a more balanced, multi-species coexistence. This equilibrium facilitates functional complementarity, thereby improving ecosystem stability in response to environmental fluctuations. The dominance of *Candidatus Solibacter* in Pan'an-transplanted groups correlates with soil acidity (Table 1).[16] Furthermore, the functional differentiation observed in the Bozhou rhizosphere—dominated by *Arthrobacter* and *Nocardioides*—reflects an adaptation to low organic matter environments. *Arthrobacter* secretes growth hormones to mitigate oxidative stress, while *Nocardioides* contributes to heavy metal detoxification[17,18] Changes in bulk soil microbiota confirm that long-term environmental filtering shapes these communities, whereas the stability of root endophytes suggests strict host selection to maintain core functions despite environmental variation. These findings support the hypothesis that the "post-transplantation reconstructed" microbial community promotes the growth of *A. macrocephala* in new environments, aligning with the established theory of "geographic adaptation through microbial community reconstruction."[19]

Microbially mediated the growth and secondary metabolism of *A. macrocephala*

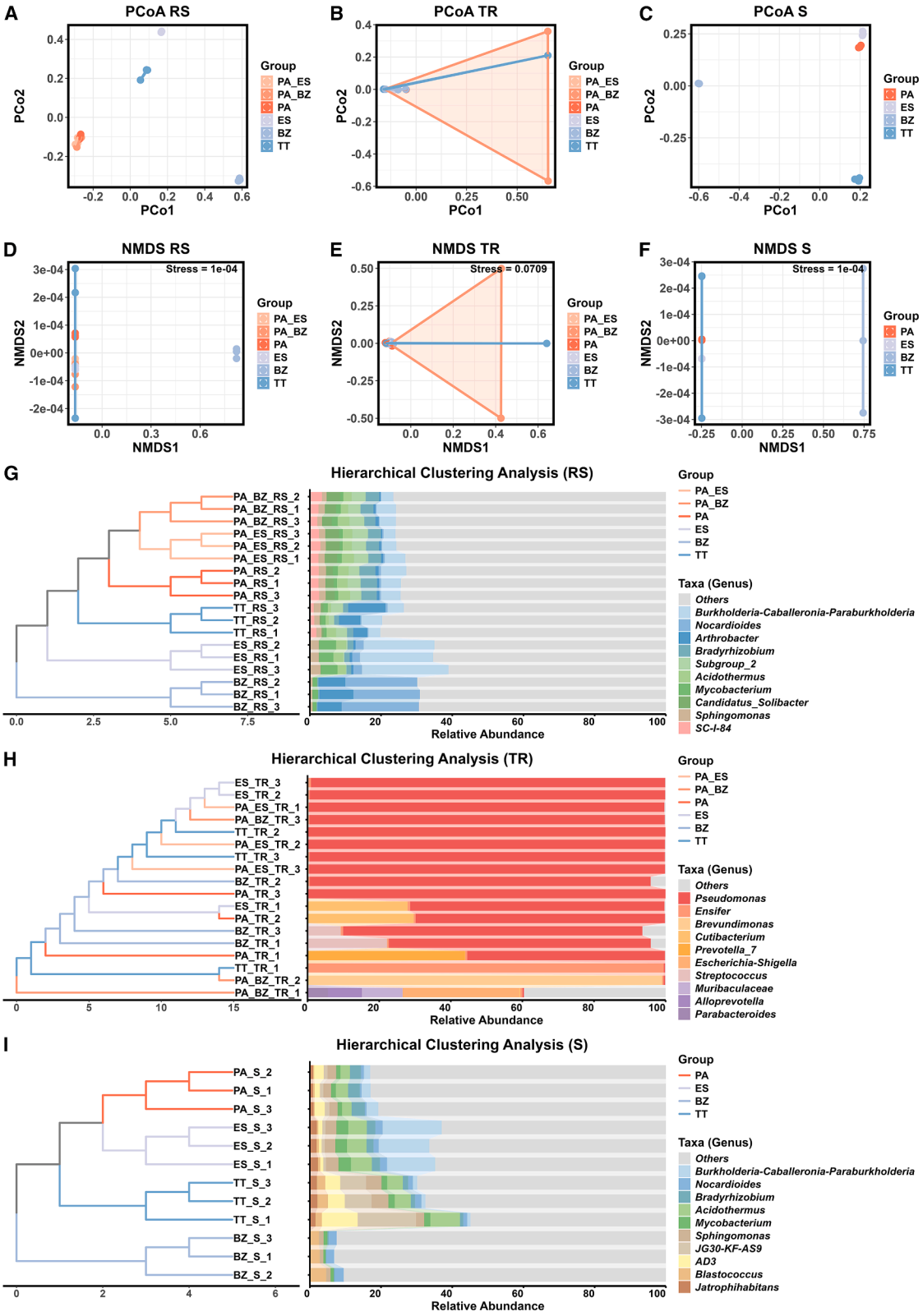
Plants prioritize energy for tissue construction over secondary metabolite synthesis under favorable ecological conditions.[20,21] The structural remodeling of the rhizosphere microbiome drives this allocation. We observed that upregulated genera in the Pan'an environment (*Anaeromyxobacter*, *Sphingomonas*, and *Sulfuritalea*) positively correlate with growth traits. *Anaeromyxobacter*, known for its nitrogen fixation and iron reduction capabilities, may indirectly promote plant metabolism by improving rhizosphere redox status and soil nitrogen availability.[22,23] *Sphingomonas* is widely recognized as a plant growth-promoting genus, its members participate in aromatic compound degradation and may modulate plant hormones, potentially regulating secondary metabolic pathways and stimulating root growth.[24,25] *Sulfuritalea* contributes to the sulfur cycle, where sulfur-oxidation activities help maintain sulfur balance and influence sulfur utilization by other organisms.[26] Its enrichment may optimize soil sulfur nutrition or affect the synthesis of sulfur-containing amino acids, providing precursors for secondary metabolic pathways and thereby indirectly influencing plant secondary metabolism. Other upregulated genera, such as *Bauldia*, *FCPS473*, *Tardiphaga*, and *JG30a-KF-32*, also showed positive correlations with plant height, root length, and specific metabolites. These genera possess diverse functional potentials: *Bauldia* may improve plant growth through metabolite regulation, *FCPS473* may be associated with nitrogen-source utilization in low-nitrogen environments, and *Tardiphaga* has been reported to exhibit heavy-metal tolerance and potential phosphorus-related enzyme synthesis.[27–30] Collectively, after transplantation to Pan'an, the upregulated rhizosphere bacterial genera likely promoted plant growth by participating in nitrogen, sulfur, and phosphorus cycling, as well as hormone-regulation pathways, serving as key drivers of improved agronomic traits in *A. macrocephala*.

In contrast, downregulated genera predominantly belonged to the phylum Actinobacteria (*Actinoplanes*, *Glycomyces*, and *Saccharopolyspora*), which are typically recognized for their potential to produce antibiotics, degrade complex organic matter, or promote plant growth.[31–33] In the original habitat (Bozhou), these genera may have established balanced or beneficial interactions with *A. macrocephala*, for instance by providing bioactive substances (e.g., plant-hormone analogs or other inducing factors), participating in key nutrient transformations, or indirectly enhancing plant resistance, thereby contributing to the basal accumulation of secondary metabolites.[34–37]

Following transplantation to Pan'an, however, the unique soil environment (including its physicochemical properties and native microbiome) may no longer support or require the original functions of these genera. Their presence could even lead to competition or functional conflict with the locally adapted, growth-promoting microorganisms. Consequently, these originally beneficial genera were largely replaced by more efficient, Pan'an-adapted microbes that provide superior growth conditions, resulting in a marked decline in their abundance. The association between their reduced abundance and higher bioactive-compound levels in Pan'an-grown *A. macrocephala* likely reflects the overall superior functionality of the Pan'an-native dominant microbial community, rather than a direct inhibitory effect of the downregulated genera themselves. This shift represents an ecological niche replacement and functional

Figure 5. Alpha diversity of soil and rhizosphere soil microorganisms of *Atractylodes macrocephala* in different regions

All the experiments were performed with three replicates. Differences between groups were assessed for significance using the Kruskal-Wallis test (for multiple groups) or the Wilcoxon rank-sum test (for two groups). (A) rhizosphere soil (RS) microorganisms; (B) tuberous root (TR) microorganisms; (C) bulk soil (S) microorganisms; PA_ES, Enshi samples planted in the Pan'an common garden; PA_BZ, Bozhou samples planted in the Pan'an common garden; PA, Pan'an; ES, Enshi; BZ, Bozhou; TT, Tiantai.



(legend on next page)

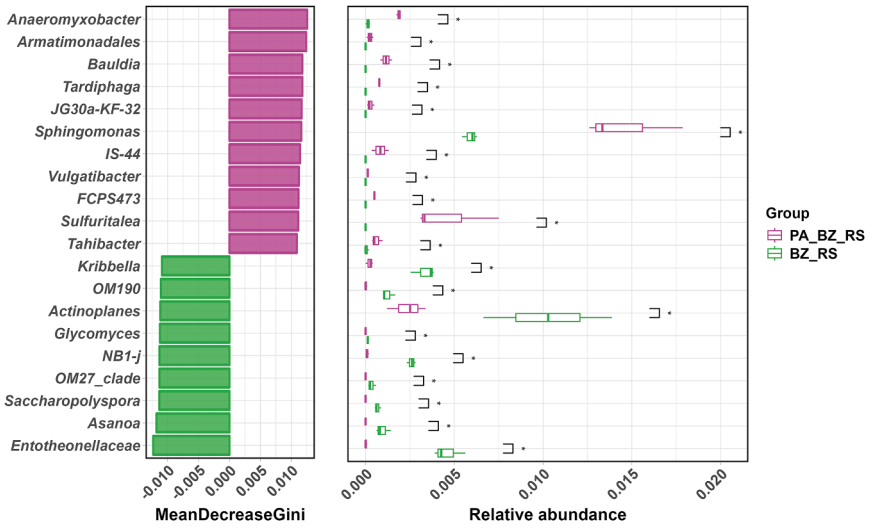


Figure 7. Random forest analysis revealed differential bacterial genera with significant contributions to classification

The left panel shows the ranking of microbial importance in the classification model (Mean Decrease Gini), while the right panel displays boxplots of the relative abundances of the corresponding bacterial genera in the two sample groups (PA_BZ_RS vs. BZ_RS). Asterisks indicate statistically significant differences between the two groups ($p < 0.05$).

optimization, wherein the Pan'an environment selected a more adapted and efficient microbial consortium to support plant growth and metabolism.

In summary, significant correlations exist between key rhizosphere bacterial genera and the phenotypic traits/medicinal components of *A. macrocephala* after transplantation to Pan'an. These findings highlight the crucial role of rhizosphere microbial community functional optimization and niche replacement in plant adaptation to new environments. Although further experimental validation of the specific mechanisms is needed, preliminary evidence supports the hypothesis that structural remodeling is a key ecological factor through which the rhizosphere microbiome participates in regulating post-transplantation growth improvement and quality formation in *A. macrocephala*. This phenomenon of microbial community restructuring driving plant phenotypic changes has also been reported in studies of other medicinal plants. For example, Zhang et al.[38] investigated changes in rhizosphere bacterial communities in tomatoes transplanted into different cultivation substrates and reported that post-transplantation bacterial community structure and abundance converged toward the characteristics of the soil community, with functional differences observed across environments. Bziuk et al.[39] reported that changes in the rhizosphere microbiome significantly enhanced powdery mildew resistance in greenhouse-cultivated barley, reducing lesion numbers and activating defense genes. In the new environment, significant microbial community turnover occurs, enriching bacterial groups that are more beneficial to plant growth and metabolism while reducing the proportion of some members from the original habitat community. This ultimately results in the formation of a rhizosphere ecosystem that is more conducive to the growth and metabolic advantages of *A. macrocephala* in PA. Importantly, this microbial structural shift is not only evident at the diversity level (Figures 5 and 6) but also manifests more profoundly as changes in functional microbial components. Functions related to nutrient cycling (sulfur, nitrogen, iron, and carbon), hormone regulation, and signaling molecule metabolism are enhanced (Figures 7 and 8).

Metabolic reprogramming supports environmental adaptation

The metabolic restructuring observed after transplantation provides the mechanistic basis for the improved growth phenotypes. The universal increase in amino acid biosynthesis underscores its role in maintaining community homeostasis.[40,41] The synthesis of cofactors and vitamins showed significant variation among different ecological niches, suggesting a regulatory function during environmental adaptation.[42] The specific upregulation of aromatic compound degradation and oxidative phosphorylation in the rhizosphere indicates efficient decomposition of root exudates.[43]

Energy metabolism also adapted to the new niche. The enhancement of butyrate fermentation and methylglyoxal degradation in tuberous roots supports diverse energy supply patterns and stress resistance.[44] The upregulation of the methylglyoxal degradation superpathway (METHGLYUT-PWY) further supports enhanced sugar metabolism efficiency and stress resistance in the PA environment.[45,46] Furthermore, the downregulation of stress-related pathways (e.g., coumarin biosynthesis) implies that the Pan'an environment imposes less survival pressure on the microbiome.[47,48] Conversely, the upregulation of enterobactin biosynthesis suggests a specialized iron acquisition mechanism essential for the rapid growth observed in Pan'an.[49] Collectively, these metabolic shifts confirm that the microbiome

Figure 6. PCoA of soil and rhizosphere soil microorganisms of *Atractylodes macrocephala* in different regions

(A) rhizosphere soil, RS; (D) tuberous root, TR; (G) bulk soil, S, NMDS analysis (B) RS; (E) TR; (H) S, and hierarchical clustering analysis (C) RS; (F) TR; (I) S of beta diversity. PERMANOVA (999 permutations) was used to assess the explanatory power (R^2) and significance (p value) of group differences, supplemented by ANOSIM for validation.

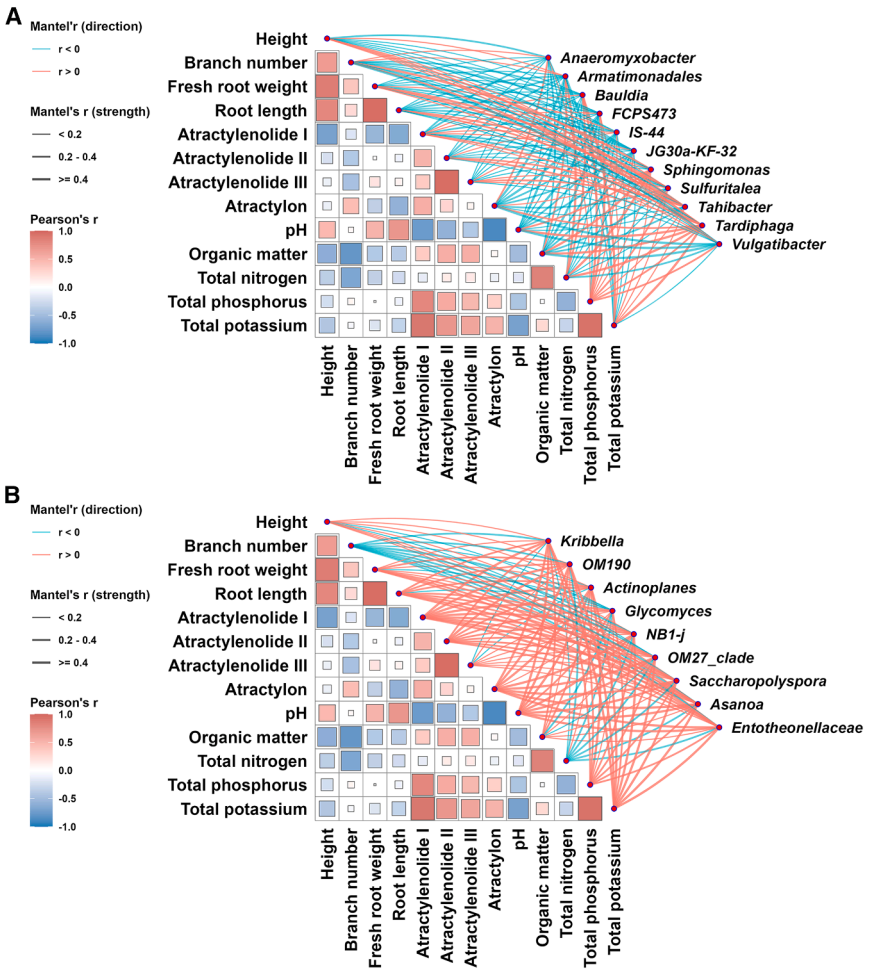


Figure 8. Network diagram of the correlation between rhizosphere microorganisms and phenotypic traits, as well as active components of *Atractylodes macrocephala*

The lower left section displays a heatmap of the Pearson correlation coefficients between agronomic traits and major metabolic components of *A. macrocephala*, where the colors indicate the direction and strength of the correlations (red, positive correlation; blue, negative correlation), and the size of the squares reflects the absolute value of the correlation coefficients. The right side presents a correlation network between differential bacterial genera and various traits/components based on Mantel test analysis. The color of connecting lines indicates the correlation direction (red, positive correlation; blue, negative correlation), whereas the line thickness represents the correlation strength (thick lines, $r \geq 0.3$; medium lines, $0.15 \leq r < 0.3$; thin lines, $r < 0.15$). Differential bacterial genera were selected through random forest screening, excluding unclassified taxa. This diagram reveals the potential role of specific microorganisms in regulating the growth, development, and accumulation of secondary metabolites in *A. macrocephala*. (A) up-regulated group; (B) down-regulated group.

undergoes adaptive reprogramming to provide sufficient nutritional support, thereby driving the successful transplantation and growth enhancement of *A. macrocephala*.

In summary, through integrated multi-regional transplantation experiments, soil factor analysis, and microbiome technology, this study systematically elucidated the microecological mechanisms through which geographical environments drive phenotypic and quality variations in *A. macrocephala*. The results demonstrate that the Pan'an region, characterized by an optimal soil pH and abundant phosphorus and potassium content, significantly enhances bioactive compound accumulation in Bozhou-sourced *A. macrocephala*. Consequently, compared with those in other regions, Pan'an-transplanted plants exhibit superior growth vigor and secondary metabolite levels. Geographic migration reshaped the microbial communities, leading to a significant increase in rhizosphere microbial α-diversity. *Proteobacteria* and *Acidobacteria* emerged as the dominant phyla in the Pan'an rhizosphere, wheras the tuberous root endosphere remained dominated by *Proteobacteria*, reflecting host genetic conservatism. Functional analysis revealed that Pan'an rhizosphere microbes optimized carbon and nitrogen use efficiency by activating metabolic pathways such as aromatic compound degradation. Eleven genera, including *Anaeromyxobacter* and *Sphingomonas*, were positively correlated with plant growth and bioactive compound accumulation. Conversely, the reduction in nine genera (e.g., *Kribbella*) likely promoted metabolic resource allocation toward growth via niche replacement, revealing the regulatory role of microbes in the regulation between plant growth and secondary metabolism.

Notably, microbe-mediated resource reallocation may represent a core mechanism regulating medicinal quality—the functional restructuring of microbial consortia in Pan'an increased host energy toward secondary metabolism, resulting in a significant negative correlation between bioactive compounds and growth traits. These findings provide some insights into yield-quality synergy in the geoherbal cultivation of medicinal plants.

Limitations of the study

Although the four producing regions showed no differences in key climatic parameters such as temperature and precipitation, subtle variations in local microclimates (e.g., sunshine duration, fog frequency, or diurnal temperature range) may still exist and could potentially influence the microbial community. Furthermore, the bacterial taxa identified through our screening process have not yet been isolated and cultured for subsequent functional validation. The isolation and in-depth functional characterization of these key bacteria will be a primary focus of our future research.

Future research should deeply integrate metagenomic functional annotation with metabolic flux analysis to validate the growth-promoting genes of key genera (e.g., *Anaeromyxobacter* and *Sphingomonas*) and their molecular pathways that regulate host terpenoid synthesis, thereby clarifying plant-microbe interaction mechanisms. Concurrently, field-applicable technologies based on PA-characteristic microbial consortia, such as developing compound microbial fertilizers to directionally enhance rhizosphere functionality in geoherbal cultivation, should be explored. Furthermore, establishing a medicinal plant rhizosphere-root microbiome database that integrates environmental factors would facilitate the prediction of ecological cultivation standards. This approach could provide universal paradigms for improving the cross-regional quality of geoherbs, ultimately advancing the ecological cultivation and industrial sustainability of traditional Chinese medicinal materials.

RESOURCE AVAILABILITY

Lead contact

Requests for further information and resources should be directed to and will be fulfilled by the lead contact, Dawei Xue (dwxue@hznu.edu.cn).

Materials availability

This study did not generate new unique reagents.

Data and code availability

This study does not report original code. And the 16S rRNA gene sequencing data have been deposited at China National Center for Bioinformation, accession number (PRJCA064424) is listed in the key resources table. Any additional information required to reanalyze the data reported in this study is available from the lead contact upon request.

ACKNOWLEDGMENTS

This work was supported by funding from the HZNU Scientific Research and Innovation Team Project (TD2025005) and Key Scientific and Technological Grant of Zhejiang for Breeding New Agricultural Varieties (2021C02074).

AUTHOR CONTRIBUTIONS

Y. Ping: data curation, methodology, visualization, and writing – original draft; Y. Peng: investigation, visualization, and writing – original draft; J.S.: resources, investigation, and methodology; J. Xiang: methodology and visualization; P.W.: resources and investigation; Y.S.: resources and investigation; J. Xia: visualization; C.D.: formal analysis, visualization, and writing – review and editing; J.L.: conceptualization, project administration, and writing – review and editing; D.X.: supervision, conceptualization, and writing – review and editing.

DECLARATION OF INTERESTS

The authors declare no competing interests.

STAR★METHODS

Detailed methods are provided in the online version of this paper and include the following:

- KEY RESOURCES TABLE
- METHOD DETAILS
  - Cultivation and transplanting plan for *A. macrocephala*
  - Sample collection methods
  - Rhizosphere soil and bulk soil collection
  - Endophyte sample collection
  - Analysis method
  - 16S sequencing
  - Microbial community taxonomic analysis
  - Alpha and beta diversity analysis
  - Functional gene prediction and diversity analysis
  - Differential taxa and phenotype association and metabolic pathway analysis
- QUANTIFICATION AND STATISTICAL ANALYSIS

SUPPLEMENTAL INFORMATION

Supplemental information can be found online at https://doi.org/10.1016/j.isci.2026.116350.

Received: November 17, 2025
Revised: January 7, 2026
Accepted: May 27, 2026

REFERENCES

1. Chen, J., Yang, S., Luo, H., Fu, X., Li, W., Li, B., Fu, C., Chen, F., Xu, D., and Cao, N. (2024). Polysaccharide of atractylodes macrocephala koidz alleviates NAFLD-induced hepatic inflammation in mice by modulating the TLR4/MyD88/NF-κB pathway. Int. Immunopharmacol. *141*, 113014. https://doi.org/10.1016/j.intimp.2024.113014.
2. Fan, M., Gu, X., Zhang, W., Shen, Q., Zhang, R., Fang, Q., Wang, Y., Guo, X., Zhang, X., and Liu, X. (2022). Atractylenolide I ameliorates cancer cachexia through inhibiting biogenesis of IL-6 and tumour-derived extracellular vesicles. J. Cachexia Sarcopenia Muscle *13*, 2724–2739. https://doi.org/10.1002/jcsm.13079.
3. Niu, X., Gu, H., Li, J., Zuo, J., Ren, W., Huang, Y., Shu, X., Jiang, C., and Shu, P. (2024). Efficacy and safety of Atractylodes macrocephala-containing traditional Chinese medicine combined with neoadjuvant chemotherapy in the treatment of advanced gastric cancer: a systematic evaluation and meta-analysis. Front. Oncol. *14*, 1431381. https://doi.org/10.3389/fonc.2024.1431381.
4. Zhu, B., Zhang, Q.l., Hua, J.w., Cheng, W.l., and Qin, L.p. (2018). The traditional uses, phytochemistry, and pharmacology of Atractylodes macrocephala Koidz.: A review. J. Ethnopharmacol. *226*, 143–167. https://doi.org/10.1016/j.jep.2018.08.023.
5. Chen, L.-G., Jan, Y.-S., Tsai, P.-W., Norimoto, H., Michihara, S., Murayama, C., and Wang, C.-C. (2016). Anti-inflammatory and antinociceptive constituents of atractylodes japonica koidzumi. J. Agric. Food Chem. *64*, 2254–2262. https://doi.org/10.1021/acs.jafc.5b05841.
6. Hao, Y., Zhang, X., Lin, X., Yang, S., Huang, Y., Lai, W., Liao, X., Liao, W., Fu, C., and Zhang, Z. (2024). *the traditional Chinese medicine processing change chemical composition and pharmacological effectiveness: Taking *atractylodes macrocephala* koidz. and honey bran-fried *atractylodes macrocephala* koidz. as examples. Phytomedicine *130*, 155739. https://doi.org/10.1016/j.phymed.2024.155739.
7. Yang, R., Wang, Y., Wang, J., Guo, X., Zhao, Y., Zhu, K., Zhu, X., Zou, H., and Yan, Y. (2024). Geographical origin traceability of atractylodis macrocephalae rhizoma based on chemical composition, chromaticity, and electronic nose. Molecules *29*, 4991. https://doi.org/10.3390/molecules29214991.
8. Yang, Y., Wang, S., Bai, R., Xiong, F., Jin, Y., Liu, H., Wang, Z., Yang, C., Yu, Y., Chowdhury, A., et al. (2024). Geographic variation in secondary metabolites contents and their relationship with soil mineral elements in pleuropterus multiflorum thunb. from different regions. Sci. Tradit. Chin. Med. *2*, 214–223. https://doi.org/10.1097/st9.0000000000000036.
9. Mehalaine, S., and Chenchouni, H. (2020). Plants of the same place do not have the same metabolic pace: Soil properties affect differently essential

oil yields of plants growing wild in semiarid mediterranean lands. Arab. J. Geosci. *13*, 1263. https://doi.org/10.1007/s12517-020-06219-4.

10. Pal, G., Saxena, S., Kumar, K., Verma, A., Sahu, P.K., Pandey, A., White, J.F., and Verma, S.K. (2022). Endophytic burkholderia: Multifunctional roles in plant growth promotion and stress tolerance. Microbiol. Res. *265*, 127201. https://doi.org/10.1016/j.micres.2022.127201.
11. Tong, Y., Zheng, X., Hu, Y., Wu, J., Liu, H., Deng, Y., Lv, W., Yao, H., Chen, J., and Ge, T. (2024). Root exudate-mediated plant–microbiome interactions determine plant health during disease infection. Agric. Ecosyst. Environ. *370*, 109056. https://doi.org/10.1016/j.agee.2024.109056.
12. Ninkuu, V., Zhang, L., Yan, J., Fu, Z., Yang, T., and Zeng, H. (2021). Biochemistry of terpenes and recent advances in plant protection. Int. J. Mol. Sci. *22*, 5710. https://doi.org/10.3390/ijms22115710.
13. Su, J., Wang, Y., Bai, M., Peng, T., Li, H., Xu, H.-J., Guo, G., Bai, H., Rong, N., Sahu, S.K., et al. (2023). Soil conditions and the plant microbiome boost the accumulation of monoterpenes in the fruit of citrus reticulata 'chachi. Microbiome *11*, 61. https://doi.org/10.1186/s40168-023-01504-2.
14. Duan, M., Yang, C., Bao, L., Han, D., He, H., Zhang, Y., Dong, L., and Yang, S. (2024). Unraveling the key mechanisms of gastrodia elata continuous cropping obstacles: Soil bacteria massilia, burkholderia-caballeronia-paraburkholderia, and dyella along with soil metabolites 4-hydroxy-benzenemethanol and N-(2-butyl)-N-octadecyl-ethyl ester as crucial indicators. Front. Microbiol. *15*, 1478330. https://doi.org/10.3389/fmicb.2024.1478330.
15. Ong, A., and O'Brian, M.R. (2024). Bradyrhizobium japonicum (diazoefficiens). Trends Microbiol. *32*, 614–615. https://doi.org/10.1016/j.tim.2024.03.010.
16. Jones, R.T., Robeson, M.S., Lauber, C.L., Hamady, M., Knight, R., and Fierer, N. (2009). A comprehensive survey of soil acidobacterial diversity using pyrosequencing and clone library analyses. ISME J. *3*, 442–453. https://doi.org/10.1038/ismej.2008.127.
17. AbdElgawad, H., Zinta, G., Abuelsoud, W., Hassan, Y.M., Alkhalifah, D.H.M., Hozzein, W.N., Zrieq, R., Beemster, G.T., and Schoenaers, S. (2021). An actinomycete strain of *nocardiopsis lucentensis* reduces arsenic toxicity in barley and maize. J. Hazard. Mater. *417*, 126055. https://doi.org/10.1016/j.jhazmat.2021.126055.
18. Jiang, Y., Song, Y., Jiang, C., Li, X., Liu, T., Wang, J., Chen, C., and Gao, J. (2022). Identification and characterization of arthrobacter nicotinovorans JI39, a novel plant growth-promoting rhizobacteria strain from panax ginseng. Front. Plant Sci. *13*, 873621. https://doi.org/10.3389/fpls.2022.873621.
19. Wang, S., Bao, X., Feng, K., Deng, Y., Zhou, W., Shao, P., Zheng, T., Yao, F., Yang, S., Liu, S., et al. (2021). Warming-driven migration of core microbiota indicates soil property changes at continental scale. Sci. Bull. *66*, 2025–2035. https://doi.org/10.1016/j.scib.2021.01.021.
20. Han, W.-H., Zhang, F.-B., Ji, S.-X., Liang, K.-L., Wang, J.-X., Fan, X.-P., Liu, S.-S., and Wang, X.-W. (2025). Auxin-salicylic acid seesaw regulates the age-dependent balance between plant growth and herbivore defense. Sci. Adv. *11*, eadu5141. https://doi.org/10.1126/sciadv.adu5141.
21. Liu, R., Yang, X., Gao, R., Hou, X., Huo, L., Huang, Z., and Cornelissen, J.H.C. (2021). Allometry rather than abiotic drivers explains biomass allocation among leaves, stems and roots of artemisia across a large environmental gradient in China. J. Ecol. *109*, 1026–1040. https://doi.org/10.1111/1365-2745.13532.
22. Masuda, Y., Yamanaka, H., Xu, Z.-X., Shiratori, Y., Aono, T., Amachi, S., Senoo, K., and Itoh, H. (2020). Diazotrophic anaeromyxobacter isolates from soils. Appl. Environ. Microbiol. *86*, e00956-20. https://doi.org/10.1128/AEM.00956-20.
23. Tang, R., Yang, S., Narsing Rao, M.P., Xie, C.-J., Han, S., Yang, Q.-E., Rensing, C., Liu, G.-H., Yuan, Y., and Zhou, S.-G. (2024). Three fe(III)-reducing and nitrogen-fixing bacteria, anaeromyxobacter terrae sp. nov., anaeromyxobacter oryzisoli sp. nov. and anaeromyxobacter soli sp. nov., isolated from paddy soil. Int. J. Syst. Evol. Microbiol. *74*, 006268. https://doi.org/10.1099/ijsem.0.006268.
24. Asaf, S., Numan, M., Khan, A.L., and Al-Harrasi, A. (2020). Sphingomonas: From diversity and genomics to functional role in environmental remediation and plant growth. Crit. Rev. Biotechnol. *40*, 138–152. https://doi.org/10.1080/07388551.2019.1709793.
25. Mazoyon, C., Catterou, M., Alahmad, A., Mongelard, G., Guénin, S., Sarazin, V., Dubois, F., and Duclercq, J. (2023). Sphingomonas sediminicola Dae20 is a highly promising beneficial bacteria for crop biostimulation due to its positive effects on plant growth and development. Microorganisms *11*, 2061. https://doi.org/10.3390/microorganisms11082061.
26. Watanabe, T., Kojima, H., and Fukui, M. (2014). Complete genomes of freshwater sulfur oxidizers *sulfuricella denitrificans* skB26 and *sulfuritalea hydrogenivorans* sk43H: Genetic insights into the sulfur oxidation pathway of betaproteobacteria. Syst. Appl. Microbiol. *37*, 387–395. https://doi.org/10.1016/j.syapm.2014.05.010.
27. Bao, Z., Wang, C., Cao, J., Zhang, T., Guo, Y., Sato, Y., Nishizawa, T., and Ohta, H. (2024). Tardiphaga alba sp. nov., a heavy-metal-tolerant bacterium isolated from garden soil. Int. J. Syst. Evol. Microbiol. *74*, 006238. https://doi.org/10.1099/ijsem.0.006238.
28. Deng, P., Zhou, Y., Chen, W., Tang, F., and Wang, Y. (2024). Microbial mechanisms for improved soil phosphorus mobilization in monoculture conifer plantations by mixing with broadleaved trees. J. Environ. Manage. *359*, 120955. https://doi.org/10.1016/j.jenvman.2024.120955.
29. Wang, X., Wang, Y., Fu, Y., Zhai, Y., Bai, X., Liu, T., Li, G., Zeng, L., and Zhu, S. (2024). Multiple omics revealed the growth-promoting mechanism of bacillus velezensis strains on ramie. Front. Plant Sci. *15*, 1367862. https://doi.org/10.3389/fpls.2024.1367862.
30. Yang, S., Xiao, J., Liang, T., He, W., and Tan, H. (2021). Response of soil biological properties and bacterial diversity to different levels of nitrogen application in sugarcane fields. AMB Express *11*, 172. https://doi.org/10.1186/s13568-021-01331-4.
31. Chukwuneme, C.F., Babalola, O.O., Kutu, F.R., and Ojuederie, O.B. (2020). Characterization of actinomycetes isolates for plant growth promoting traits and their effects on drought tolerance in maize. J. Plant Interact. *15*, 93–105. https://doi.org/10.1080/17429145.2020.1752833.
32. Mitra, D., Mondal, R., Khoshru, B., Senapati, A., Radha, T.K., Mahakur, B., Uniyal, N., Myo, E.M., Boutaj, H., Sierra, B.E.G., et al. (2022). Actinobacteria-enhanced plant growth, nutrient acquisition, and crop protection: Advances in soil, plant, and microbial multifactorial interactions. Pedosphere *32*, 149–170. https://doi.org/10.1016/S1002-0160(21)60042-5.
33. Xu, T., Xi, J., Ke, J., Wang, Y., Chen, X., Zhang, Z., and Lin, Y. (2023). Deciphering soil amendments and actinomycetes for remediation of cadmium (cd) contaminated farmland. Ecotoxicol. Environ. Saf. *249*, 114388. https://doi.org/10.1016/j.ecoenv.2022.114388.
34. Berendsen, R.L., Pieterse, C.M.J., and Bakker, P.A.H.M. (2012). The rhizosphere microbiome and plant health. Trends Plant Sci. *17*, 478–486. https://doi.org/10.1016/j.tplants.2012.04.001.
35. de Faria, M.R., Costa, L.S.A.S., Chiaramonte, J.B., Bettiol, W., and Mendes, R. (2020). The rhizosphere microbiome: Functions, dynamics, and role in plant protection. Trop. plant pathol. *46*, 13–25. https://doi.org/10.1007/s40858-020-00390-5.
36. Gu, Y., Yan, W., Chen, Y., Liu, S., Sun, L., Zhang, Z., Lei, P., Wang, R., Li, S., Banerjee, S., et al. (2025). Plant growth-promotion triggered by extracellular polymer is associated with facilitation of bacterial cross-feeding networks of the rhizosphere. Isme J *19*, wraf040. https://doi.org/10.1093/ismejo/wraf040.
37. Li, Q., Liu, Z., Jiang, Z., Jia, M., Hou, Z., Dou, D., and Yu, J. (2025). Phenylalanine metabolism-dependent lignification confers rhizobacterium-induced plant resistance. Plant Physiol. *197*, kiaf016. https://doi.org/10.1093/plphys/kiaf016.
38. Zhang, X., Li, Q., Zhou, F., Fan, S., Zhao, X., Zhang, C., Yan, K., and Wu, X. (2023). Effects of different cultivation media on root bacterial community

characteristics of greenhouse tomatoes. Front. Microbiol. *14*, 1182347. https://doi.org/10.3389/fmicb.2023.1182347.

39. Bziuk, N., Maccario, L., Sørensen, S.J., Schikora, A., and Smalla, K. (2022). Barley rhizosphere microbiome transplantation – a strategy to decrease susceptibility of barley grown in soils with low microbial diversity to powdery mildew. Front. Microbiol. *13*, 830905. https://doi.org/10.3389/fmicb.2022.830905.
40. Fitzpatrick, C.R., Salas-González, I., Conway, J.M., Finkel, O.M., Gilbert, S., Russ, D., Teixeira, P.J.P.L., and Dangl, J.L. (2020). The plant microbiome: From ecology to reductionism and beyond. Annu. Rev. Microbiol. *74*, 81–100. https://doi.org/10.1146/annurev-micro-022620-014327.
41. Zhalnina, K., Louie, K.B., Hao, Z., Mansoori, N., da Rocha, U.N., Shi, S., Cho, H., Karaoz, U., Loqué, D., Bowen, B.P., et al. (2018). Dynamic root exudate chemistry and microbial substrate preferences drive patterns in rhizosphere microbial community assembly. Nat. Microbiol. *3*, 470–480. https://doi.org/10.1038/s41564-018-0129-3.
42. Levy, A., Salas Gonzalez, I., Mittelviefhaus, M., Clingenpeel, S., Herrera Paredes, S., Miao, J., Wang, K., Devescovi, G., Stillman, K., Monteiro, F., et al. (2018). Genomic features of bacterial adaptation to plants. Nat. Genet. *50*, 138–150. https://doi.org/10.1038/s41588-017-0012-9.
43. Kuzyakov, Y., and Blagodatskaya, E. (2015). Microbial hotspots and hot moments in soil: Concept & review. Soil Biol. Biochem. *83*, 184–199. https://doi.org/10.1016/j.soilbio.2015.01.025.
44. Brame, J.E., Liddicoat, C., Abbott, C.A., Edwards, R.A., Robinson, J.M., Gauthier, N.E., and Breed, M.F. (2024). The macroecology of butyrate-producing bacteria via metagenomic assessment of butyrate production capacity. Ecol. Evol. *14*, e11239. https://doi.org/10.1002/ece3.11239.
45. Kaur, C., Sharma, S., Singla-Pareek, S.L., and Sopory, S.K. (2016). Methylglyoxal detoxification in plants: Role of glyoxalase pathway. Indian J. Plant Physiol. *21*, 377–390. https://doi.org/10.1007/s40502-016-0260-1.
46. Shivani, Grewal, S.K., Grewal, S.K., Gill, R.K., Virk, H.K., and Bhardwaj, R.D. (2022). Methylglyoxal detoxification pathway - explored first time for imazethapyr tolerance in lentil (*lens culinaris* L.). Plant Physiol. Biochem. *177*, 10–22. https://doi.org/10.1016/j.plaphy.2022.02.007.
47. Bourgaud, F., Hehn, A., Larbat, R., Doerper, S., Gontier, E., Kellner, S., and Matern, U. (2006). Biosynthesis of coumarins in plants: A major pathway still to be unravelled for cytochrome P450 enzymes. Phytochem. Rev. *5*, 293–308. https://doi.org/10.1007/s11101-006-9040-2.
48. Sasse, J., Martinoia, E., and Northen, T. (2018). Feed your friends: Do plant exudates shape the root microbiome? Trends Plant Sci. *23*, 25–41. https://doi.org/10.1016/j.tplants.2017.09.003.
49. Pakarian, P., and Pawelek, P.D. (2016). Subunit orientation in the *escherichia coli* enterobactin biosynthetic EntA-EntE complex revealed by a two-hybrid approach. Biochimie *127*, 1–9. https://doi.org/10.1016/j.biochi.2016.04.007.
50. Kim, J.-H., Doh, E.-J., and Lee, G. (2016). Evaluation of medicinal categorization of atractylodes japonica koidz. by using internal transcribed spacer sequencing analysis and HPLC fingerprinting combined with statistical tools. Evid.-Based Complement. Altern. Med. Ecam *2016*, 2926819. https://doi.org/10.1155/2016/2926819.
51. Douglas, G.M., Maffei, V.J., Zaneveld, J.R., Yurgel, S.N., Brown, J.R., Taylor, C.M., Huttenhower, C., and Langille, M.G.I. (2020). PICRUSt2 for prediction of metagenome functions. Nat. Biotechnol. *38*, 685–688. https://doi.org/10.1038/s41587-020-0548-6.
52. Louca, S., and Doebeli, M. (2018). Efficient comparative phylogenetics on large trees. Bioinformatics *34*, 1053–1055. https://doi.org/10.1093/bioinformatics/btx701.
53. Ye, Y., and Doak, T.G. (2009). A parsimony approach to biological pathway reconstruction/inference for genomes and metagenomes. PLoS Comput. Biol. *5*, e1000465. https://doi.org/10.1371/journal.pcbi.1000465.
54. Paulson, J.N., Stine, O.C., Bravo, H.C., and Pop, M. (2013). Differential abundance analysis for microbial marker-gene surveys. Nat. Methods *10*, 1200–1202. https://doi.org/10.1038/nmeth.2658.

STAR★METHODS

KEY RESOURCES TABLE

REAGENT or RESOURCE	SOURCE	IDENTIFIER
Deposited data		
16S rRNA gene sequencing data	China National Center for Bioinformation	PRJCA064424 https://ngdc.cncb.ac.cn/bioproject/browse/PRJCA064424
Software and algorithms		
R	R Development Core Team, 2015	https://www.r-project.org/

METHOD DETAILS

Cultivation and transplanting plan for *A. macrocephala*

Field cultivation of *A. macrocephala* was conducted in four distinct ecological regions: Tiantai (Zhejiang), Pan'an (Zhejiang), Bozhou (Anhui), and Enshi (Hubei). Additionally, plant samples collected from Bozhou and Enshi were transplanted to a common garden in Pan'an (Zhejiang) for cultivation under uniform and controlled conditions. The detailed geographical locations of the transplant sites are provided in Table S1.

Seedlings for transplanting were selected from plants with consistent growth periods and conditions across the different source regions. At the transplanting stage, the aboveground parts had withered, and the plants showed no signs of disease. The root systems were well-developed, and the rhizomes were plump without shrinkage. Fibrous roots were trimmed to 2–3 cm in length, and the individual seedling weight was controlled within the range of 15–25 grams. All seedlings were excavated from their respective source regions between January 5 and 10, 2022, transported to Pan'an at 4°C, and uniformly transplanted on January 15, 2022. They were then subjected to identical field management practices until harvest on December 30, 2022.

Sample collection methods

Plant and rhizosphere soil sampling from cultivation areas

Sampling was performed during consecutive rain-free days. Sampling locations within target plots were determined using the five-point sampling method. Plants were carefully excavated by digging around the outer edge of the root system to obtain intact root balls with adhering rhizosphere soil, avoiding vigorous shaking. Each plant (or sampling unit) along with its rhizosphere soil was placed into a sterile bag, immediately transferred to a cooler (0–4°C) for transport, and delivered to the laboratory on the same day. Within each sampling area, 15 *A. macrocephala* plants were randomly excavated. The rhizosphere materials from these 15 plants were pooled to form one independent biological replicate. At least three such composite replicates were collected from each target plot.

Rhizosphere soil and bulk soil collection

In the laboratory, soil loosely adhering to the roots was gently brushed off and collected as rhizosphere soil. Soil samples from multiple roots were combined to form a composite rhizosphere soil sample. This pooling process was repeated three times, and the samples were stored at -20°C. For bulk soil collection, areas in the field far from *A. macrocephala* plants were randomly selected, and soil was collected using 50 mL centrifuge tubes, with three tubes collected per plot.

Endophyte sample collection

Tuberous roots of *A. macrocephala* were cut with scissors and placed into 50 mL centrifuge tubes (6 tubes total). Samples were rinsed with tap water and then transferred to new 50 mL centrifuge tubes. Under a laminar flow hood, surface sterilization was performed sequentially: immersion in 70% ethanol for 1–2 minutes, followed by immersion in 2.5% sodium hypochlorite for 5–10 minutes, and then rinsing 4–5 times with sterile water. A 500 μL aliquot of the final rinse was spread onto an antibiotic-free LB agar plate and incubated at 37°C. If no microbial colonies grew, the surface sterilization was considered successful. The remaining sterilized root material was regarded as containing endophytes and was stored at –20°C.

Analysis method

Active compound contents and soil property analysis

Chromatographic analysis was performed according to the method of Kim et al.[50] using a Hypersil GOLD C18 column (4.6 mm × 250 mm, 5 μm). The mobile phase consisted of acetonitrile and 0.1% phosphoric acid solution with a gradient elution program. The flow rate was 1.0 mL/min, the column temperature was maintained at 25 °C, and the injection volume was 20 μL. The

detection wavelengths were set at 276 nm for atractylenolide I and 220 nm for atractylenolides II and III. System suitability testing confirmed that the theoretical plate number for each peak was greater than 3000.

For solution preparation, reference standards of atractylenolides I, II, and III were accurately weighed and dissolved in methanol to prepare a series of standard solutions with concentrations ranging from 5 to 80 μg/mL. The test sample solution was prepared by accurately weighing approximately 1.0 g of the powder, placing it in a volumetric flask, and adding 10 mL of methanol precisely. The mixture was soaked at room temperature for 1 hour, followed by ultrasonic extraction for another hour. After extraction, the weight was adjusted to compensate for any loss with methanol, and the solution was mixed well and filtered, after which the filtrate was subsequently used for analysis.

Soil physicochemical properties were analyzed by Zhejiang SEP Analytical Services Co., Ltd., where soil pH was measured using a pH meter (HJ 962-2018), soil potassium content was determined via acid digestion (LY/T 1234-2015), soil nitrogen content was analyzed using the Kjeldahl method (HJ 717-2014), total soil phosphorus content was measured via alkaline fusion–molybdenum antimony anti-spectrophotometry (HJ 632-2011), and soil organic matter content was determined via volumetric analysis (LY/T 1237-1999).

16S sequencing

Samples of tuberous roots, rhizosphere soil, and bulk soil were outsourced to Shanghai Personal Biotechnology Co., Ltd., for 16S rRNA sequencing. Total DNA was extracted from the samples, and community DNA fragments were subjected to paired-end sequencing on the Illumina platform using the primer sequences (F: AACMGGATTAGATACCCKG and R: ACGTCATCCCCACCTTCC). Denoising of the sequences was performed using the DADA2 method.

Microbial community taxonomic analysis

After unclassified sequences were removed, the ASV table was rarefied to 95% of the minimum sequencing depth across all the samples. The number of taxonomic units at the phylum, class, order, family, genus, and species levels was subsequently calculated for each sample. Afterward, the top 20 genera by average abundance were selected, and clustered heatmaps were generated using the R pheatmap package based on a Bray-Curtis distance matrix; samples were ordered by UPGMA clustering to reveal cross-regional microbial abundance distribution patterns.

Alpha and beta diversity analysis

Alpha diversity indices (seven metrics) were computed in QIIME 2 (v2019.4) with a minimum rarefaction depth of 10 and a maximum depth equivalent to 95% of the minimum sample sequencing depth over 10 iterations. The mean values at the maximum depth were used as the final alpha diversity estimate for each sample. Boxplots were generated using ggplot2 for visualization.

Based on the resampled ASV table, Bray-Curtis and Unweighted UniFrac distance matrices were computed using QIIME2, followed by Principal Coordinate Analysis (PCoA). Two-dimensional ordination plots were generated using the ape package. Non-metric Multidimensional Scaling (NMDS) was then applied to Bray-Curtis distances using the vegan package in R (stress values < 0.2 were considered valid), and UPGMA hierarchical clustering was visualized using the ggtree package, where branch lengths reflected sample similarity.

Functional gene prediction and diversity analysis

Based on the amplicon sequencing data, PICRUSt2 (v2.4.2) was used to predict the functional potential of the microbial communities.[51] First, 16S rRNA feature sequences were aligned with a reference genome database (containing >20,000 genomes) for multiple sequence alignment, after which a phylogenetic tree was constructed. The Castor algorithm[52] was used to infer the evolutionary conservation of unobserved gene functions. The Nearest Sequenced Taxon Index (NTSI) threshold for feature sequences was set to 2, and sequences with an NTSI > 2 were excluded to improve prediction accuracy. The presence of metabolic pathways was strictly inferred using MinPath, and the final outputs included functional units and metabolic pathway abundance data annotated by the MetaCyc database (v24.5).[53] The functional abundance was normalized as counts per million (CPM) to ensure cross-sample comparability. Metabolic pathways were hierarchically classified into six major categories (e.g., metabolism and genetic information processing) and 45 sub-functions based on the KEGG database, whereas MetaCyc pathways were annotated based on experimentally validated biochemical reaction networks.

Differential taxa and phenotype association and metabolic pathway analysis

An integrated machine learning and statistical testing strategy was used to analyze correlations between microbial ASVs and phenotypes. Unclassified units were removed from the resampled ASV tables, and a random forest model (random Forest package) was applied to screen for differential microbes. Using the PA_BZ_RS group and BZ_RS group as response variables and all the ASVs as predictors, 2000 decision trees (ntree = 2000) were constructed, with the number of splitting variables (mtry) optimized via 10-fold cross-validation. MeanDecreaseGini was used to quantify the importance of the ASVs, and significantly different ASVs ($p < 0.05$) were determined based on 1000 permutation tests (rfPermute package). To validate the phenotype associations, Mantel tests (linkET

package) were further performed to analyze the correlations between the ASV matrix of the top 20 genera (ranked by the MeanDecreaseGini score) and the phenotype matrices, ultimately identifying the core differential taxa and their phenotypic correlations.

QUANTIFICATION AND STATISTICAL ANALYSIS

Data for the growth phenotype and active constituents of *A.macrocephala*, and soil physicochemical properties were analyzed using one-way analysis of variance (ANOVA), and significant differences among means were further assessed with Duncan's multiple range test at a significance level of $p < 0.05$. Group differences for alpha diversity were assessed using the Kruskal-Wallis test for multiple groups or the Wilcoxon rank-sum test for two groups with a significance threshold of $p < 0.05$. As for beta diversity, PERMANOVA (with 999 permutations) was used to evaluate the explanatory power (R^2) and significance (p-value) of group differences, supplemented by ANOSIM tests to validate the differences between groups.

Functional β-diversity was assessed using Bray-Curtis distance matrices, and Principal Coordinate Analysis (PCoA) was performed using the R package vegan (v2.6-4) to visualize differences in functional composition between samples. A zero-inflated log-normal (ZILN) model was applied to identify differentially abundant metabolic pathways between groups using the fit Feature Model function in the R package metagenomeSeq (v1.36.0).[54] The significance threshold was set at a false discovery rate (FDR)-adjusted $p < 0.05$.